Published in the Proceedings of the 16th International Aluminum Alloys Conference (ICAA16) 2018
ISBN: 978-1-926872-41-4
by the Canadian Institute of Mining, Metallurgy & Petroleum

DEVELOPMENT OF NEW LABORATORY-SCALE TESTS TO OPTIMIZE INDUSTRIAL THERMO-MECHANICAL PROCESSING OF THICK PLATE PRODUCTS: APPLICATION TO AlCuLi ALLOYS

*Fanny Mas and Jean-Christophe Ehrström

Constellium, C-TEC
Voreppe, France
*(*Corresponding author: fanny.mas@constellium.com)*

ABSTRACT

A specific test set-up has been developed to study at the lab-scale the high-temperature behavior of aluminium alloys in conditions close to those experienced by thick plates during hot-rolling. A particular attention is paid to reproducing both the stress triaxiality and strain fields that exist in plate during rolling. In addition to standard ductility measurements by means of secondary tensile tests (STT), multi-step plane strain compression (PSC) tests have been performed to mimic hot-rolling pass schedules. Tool and sample geometries were adapted to allow low h/a ratios (h= average specimen thickness, a= tool width) and thus guarantee depressive stress conditions at the center of the specimen during most of the test. Such conditions resulting in porosity opening can then be used to investigate the impact of rolling conditions on damage evolution. The mechanical testing was combined with post-mortem high-resolution ultrasonic scans allowing to detect small amounts of damage and quantify its evolution as a function of processing parameters such as strain and temperature. The test set-up was validated on two 2050-type AlCuLi alloys with different susceptibilities to high temperature embrittlement.

KEYWORDS

Hot-rolling, Secondary tensile test, Plane strain compression, High resolution ultrasonic testing, AlCuLi alloys

INTRODUCTION

Aluminium thick plates are widely used in the aerospace industry, mainly as semi-products to be machined for internal structure parts of wings (spars, ribs) and fuselage (frame). The conversion route of such products always involves a hot-rolling step, the conditions of which (temperature, speed, pass schedule…) have to be optimized to maximize both mechanical properties and final plate quality. This goal cannot always be efficiently achieved by full-scale industrial trials as (a) cost limits the number of possible test conditions and (b) it is often difficult to change one parameter alone. That is why there is a need for laboratory-scale tests able to mimic the rolling process in terms of temperature, strain rate, stress triaxiality and deformation. Most laboratory hot-rolling mills do not adequately simulate industrial processing routes, especially in terms of heat loss, deformation speed and rolling geometry (maximum roll gap vs. work roll diameter). Concerning thick plate, it is of interest to achieve both similar deformation and L/h ratio (L=arc of contact, h=mean gauge) per pass as the industrial schedule because they are simultaneously involved in damage evolution and void closure during hot forming processes (Saby, 2014).

Plane strain compression on a servo hydraulic test machine (as SERVOTEST Thermo-Mechanical Treatment Simulator) allows controlling appropriate temperature and strain rate and has thus been widely used to simulate hot-rolling (Timothy, 1991). However, even if the main characteristic of rolling is obtained, that is deformation in plane strain, departures from this basic stress state resulting from an industrial rolling pass are not fully simulated through the sample thickness and width. In industrial rolling, the edges are subjected to tension that may results in edge cracking, often enhanced by material sensitivity to segregating elements (Thomson, 1980). Edge cracking can be studied by Secondary Tensile Tests, a method first proposed by Woodall and Schey as a mean to assess metal workability (Schey, 1979). Holes drilled into a rectangular piece of metal create a tensile stress field in the outer ligaments when subjecting the center to plane strain compression. The measurement of area reduction after failure of the ligaments was shown to be a suitable indicator to study the effect of temperature and strain rate in 5182 and 7075 aluminium alloys (Duly, 1998). The conditions for ductility loss, and especially the critical temperature beyond which ductility is expected to drop, were in good agreement with the appearance of defects during rolling, such as alligatoring and edge cracking.

Al-Cu-Li alloys, such as those of the Airware® family, are now industrially applied for structural components in several commercial aircraft thanks to their lower density, improved corrosion resistance and improved strength, fatigue and damage tolerance compromise, in comparison with conventional 2xxx and 7xxx series aluminium alloys (Lequeu, 2010). Thus, it is desirable to define the optimal thermomechanical processing window for these alloys, namely the range of process parameters that lead to a high quality product.

The present study aims to develop a laboratory-scale test able to reproduce stress triaxiality and deformation fields encountered at different positions within a plate during hot rolling and to assess the impact of deformation conditions on damage evolution. In addition a post-mortem characterization technique allowing a quantification of small amounts of porosity is presented. Both optical micrography (2D) and X-ray tomography (3D but on millimeter-size volumes) were considered unsuitable. High-resolution ultrasonic scans on initial and deformed specimens are performed and the newly developed procedure is validated on 2050-type alloys.

MATERIALS AND METHODS

Materials

2050-type alloys were used for this study (see composition in Table 1), samples being extracted from industrial slabs after stress-relief. Homogenization treatment at temperatures around 500°C was performed in a laboratory furnace.

Table 1. 2050 composition (AA registration)

	Si	Fe	Cu	Mn	Mg	Zn	Ti	Zr	Ag	Li
AA2050	*<0.08*	*<0.10*	*3.2 - 3.9*	*0.20 - 0.50*	*0.20 - 0.60*	*<0.25*	*<0.10*	*0.06 - 0.14*	*0.20 - 0.70*	*0.7 - 1.3*

Within the 2050 family, two variants A and B were considered in this work. In comparison with alloy A, alloy B contains small amounts of vanadium. The alloys differ by their flow stress at high temperature, alloy A being slightly softer than alloy B when tested at 495°C, as shown in Figure 1.

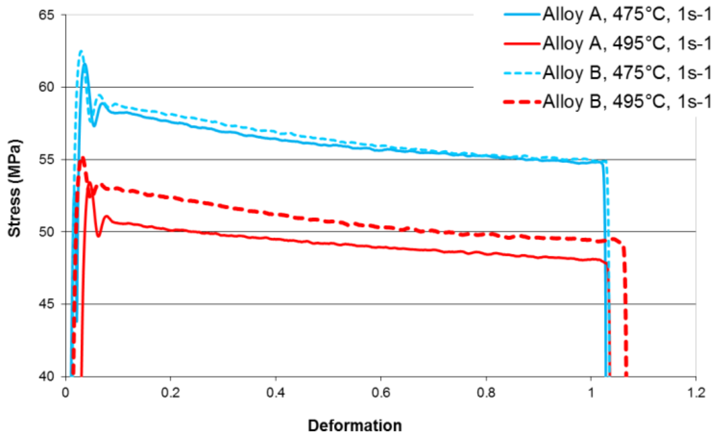

Figure 1. Flow stress evolution during plane strain compression performed on SERVOTEST TMTS (28 mm wide tool) at a constant strain rate of $1s^{-1}$.

Testing Details

Two kinds of tests were performed on a servo-hydraulic high speed SERVOTEST TMTS machine: Secondary Tensile Tests and Plane Strain Compression tests.

Secondary Tension Tests (STT)

STT were performed on alloys A and B according to the procedure described in (Duly, 1998). The samples are 80 mm in length, 65 mm in width and 20 mm in thickness. 10 mm diameter holes are drilled through thickness and reamed to leave a test ligament of width 5mm and height 20 mm. A thermocouple is centrally embeded into each sample to start the test once the specimen reaches the targeted temperature. Ductility is then measured by optical microscopy as the reduction of ligament section area and the strain to failure is defined as $\ln(S_0/S_f)$ where S_0 (resp. S_f) is the initial (resp. final) section area. Given the holes, the stress state in the ligament is close to pure tension with a triaxiality ratio (σ_m/σ_0, σ_0 being the flow stress in uniaxial tension and σ_m the hydrostatic stress) around 1/3 or above. In comparison with rolling, the deformation level that can be reached before failure is limited.

Plane strain compression (PSC) tests with high h/a ratio

Notched tensile specimens with different radii are commonly used to obtain various stress triaxiality ratios (Ehrström, 1989). In Ehrström (1989), stress triaxility ratios for aluminium alloys at high temperature are computed for two geometries: AE10 (notch radius = 5 mm) and AE4 (notch radius = 2 mm) for a 9 mm diameter bar with a 5 mm minimum diameter. DENT specimens with sharp notches have also been used to characterize high temperature tearing resistance (Chéhab, 2006). However they are thin specimens corresponding to plane stress conditions with a triaxiality ratio close to 0.6. Torsion experiments are also commonly used to study microstructural evolutions during hot-rolling as they allow large amounts of deformation before failure. However this loading mode leads to a highly heterogeneous strain along the radius of the specimen and the latter is not subjected to any hydrostatic pressure. It has been used to quantify ductily loss associated with the addition of Cu in AA5182 and to find optimized pre-heat conditions to postpone failure (Ratchev, 1997).

The specificity of hot-rolling is the variation of triaxiality and deformation for each pass along the schedule. In Figure 3, the maximum stress triaxiality calculated by FEM for a typical industrial schedule is plotted as a function of L/h ratio. At mid-width, compressive stress fields prevail above L/h=0.4. On the contrary, the edges are mainly subjected to a positive stress triaxiality (between 0.1 and 0.5) during most of the rolling schedule.

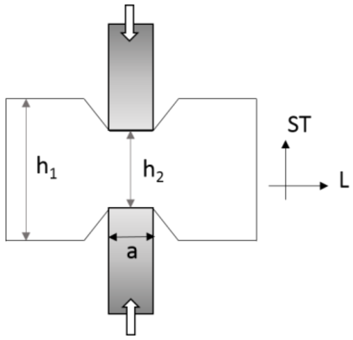

Figure 2. Notation regarding the geometry in plane strain compression.

In the case of plane strain compression, both horizontal slices and slip lines methods for rigid perfectly plastic materials are used to derive the stress triaxiality for different a/h ratios (see Figure 2 for notations). Plane strain compression with low a/h (thick specimen versus tool width) appears as a better choice than tensile specimens of various geometries for observing damage during hot-rolling. Their dimensions can be adjusted to cover the range of stress triaxiality encountered during rolling. A multi-step experiment to be carried out with the PSC machine and a 15 mm wide tool was designed. Three deformation steps were chosen with different deformation speeds in order to simulate the increase of strain rate encountered during rolling. Analytical calculations based on the simple Rice and Tracey equation for cavity growth (see equation 1 below) are used for assessing porosity opening/closure efficiency of each pass (see results in Table 2):

$$\frac{dr}{r} = 0.558 * d\varepsilon * \sinh\left(\frac{3}{2} * \frac{\sigma_m}{\sigma_0}\right) \tag{1}$$

The first two passes with triaxiality ratios between 0.15 and 0.4 should lead to porosity opening (dr/r > 0). According to the slip lines method, the first pass should give 8.4% increase in pore radius, meaning about 25% increase in volume.

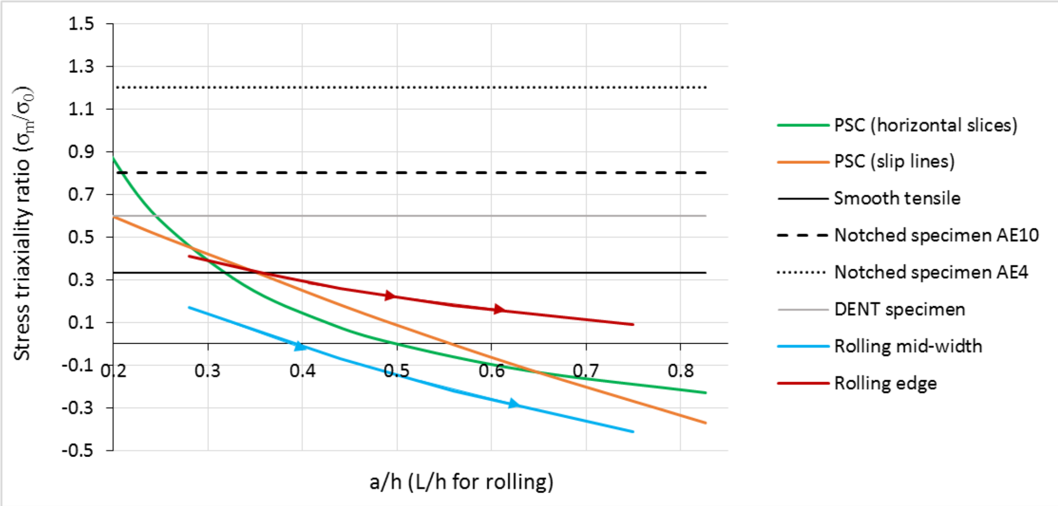

Figure 3. Comparison between industrial rolling and laboratory experiments with different geometries in terms of triaxiality versus a/h ratio. Triaxiality ratios pertaining to the above-mentioned tensile specimens have been added for comparison.

Table 2. Deformation parameters for the multi-step Servotest experiment with low a/h ratios and calculated triaxiality and pore radius variation for each pass according to both horizontal slices and slip lines methods.

Pass number	1	2	3
h1 (mm)	50	40	33
h2 (mm)	40	33	25
Δh (mm)	10	7	8
a/h	0.33	0.41	0.52
Δε	0.26	0.22	0.32
σ_m/σ_0 (horizontal slices)	0.29	0.13	-0.02
dr/r (horizontal slices)	0.064	0.023	-0.005
σ_m/σ_0 (slip lines)	0.37	0.22	0.04
dr/r (slip lines)	0.084	0.042	0.012
$\dot{\varepsilon}$ (s^{-1})	1.47	1.89	2.44

High-Resolution Ultrasonic Testing (HR-UT)

The HR-UT set-up is made of a water tank and a focused transducer (diameter of 0.5”) operating at a frequency of 15 MHz. The apparatus is calibrated in amplitude with a flat bottom hole of diameter 300 µm located at a distance of 6 mm under the metal surface. After compression, the central part of each specimen under the punch is extracted and symmetrically machined down to 16 mm thickness in the LT-ST plane. This configuration allows receiving a signal from a volume spanning 4 mm in depth (L direction) perfectly centered under the punch. The transducer is then moved above the specimen with a step of 0.28 mm in order to cover the whole LT-ST plane. The reflected amplitude mainly depends on the defect size. The C-scan, which is a map of the maximum amplitude at each position of the LT-ST plane, is the most common representation of the results (see examples in Figure 6). Such a method allows probing a sufficiently large volume (full width × full thickness × 4 mm in length) without any bias arising from either a 2D section or limited specimen size. Initial quality is assessed by scanning the un-deformed specimen ends; it was verified not to be affected by the level of deformation in the central part.

TEST RESULTS

Secondary Tensile Tests (STT)

The results obtained at different temperatures for alloys A and B are presented in Figure 4, where ductility is quantified by the $\ln(S_0/S_f)$ parameter previously defined. Although both alloys display similar ductilities at 475°C, alloy B has a more pronounced ductility loss at higher temperatures. Some of the specimens were polished in the L-ST plane in order to image damage evolution at the center of the ligament from the fracture surface towards the unaffected specimen end. Figure 5 represents the surface fraction of voids as a function of ligament height for two specimens of alloy A deformed at different temperatures. The difference in ductility is illustrated by the difference in minimum ligament height, as alloy B fractured at a smaller amount of deformation. In addition, for the same ligament height, meaning the same amount of local deformation, a larger amount of damage is measured at 515°C than at 475°C. As the number of voids is similar for both temperatures (not shown here), this result highlights a faster damage growth at 515°C.

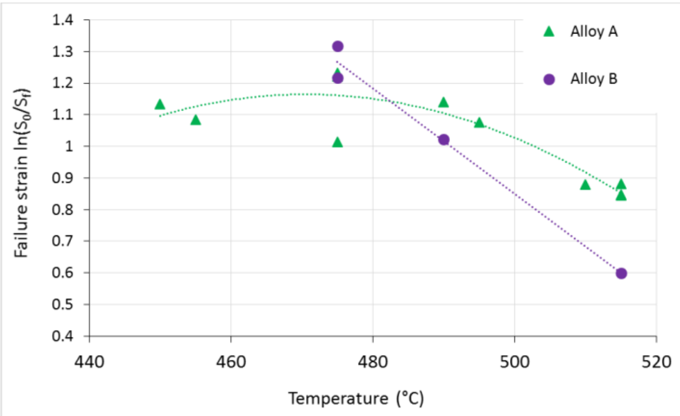

Figure 4. STT results of tests performed at different temperature for a strain rate of $1s^{-1}$ in the specimen center.

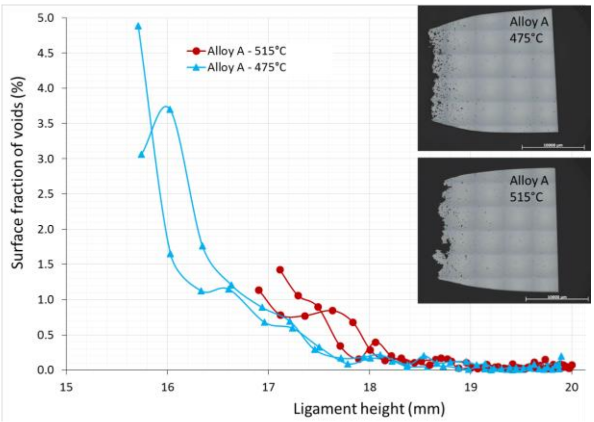

Figure 5. Results of void quantification for different positions along the ligament length by image analysis on optical micrographs.

Plane Strain Compression (PSC) Tests with High h/a Ratio

HR-UT scans in the TL-TC planes are shown in Figure 6 for alloy B deformed at 495°C in three passes as described in the previous section. Red and yellow indications (amplitude above 45%) are visible after the three levels of reduction (left edges should not be considered as they correspond to the thermocouple location). A lower level of indications was present in the initial state, meaning that either void nucleation or growth has happened in the tested conditions (alloy B, 495°C).

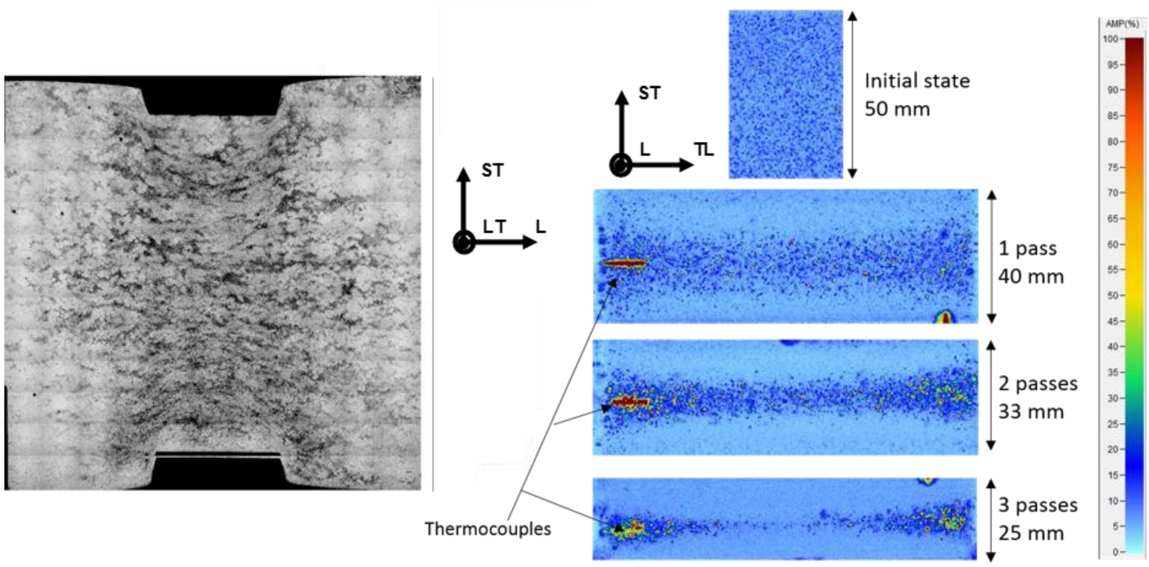

Figure 6. Macroscopic view of a plane strain compression tested specimen (left) and of HR-UT C-scans after 3 successive passes (down to 40, 33 and 25 mm thickness from an initial thickness of 50 mm).

For each deformation condition (reduction, alloy, temperature), a quantitative treatment was applied to the HR-UT C-scans, as can be seen in Figure 7 where the decreasing cumulative frequency of indications is plotted for each amplitude level. A central zone of 35 mm in TL direction that excludes both edges is selected on each sample. The initial level is represented as a dotted line. When the curve obtained after deformation lies above the curve measured in the initial condition the fraction of voids with a size greater than a certain level (represented by the amplitude percentage) has been increased. In the case of alloy A, the first pass leads to a significant void opening whereas the two following passes correspond to a decrease of the HR-UT signal at high amplitude. The final state (after pass 3) is better than the initial quality. The case of alloy B is slightly different as the second pass creates even more damage whereas porosity closure only happens between the 2nd and the 3rd passes.

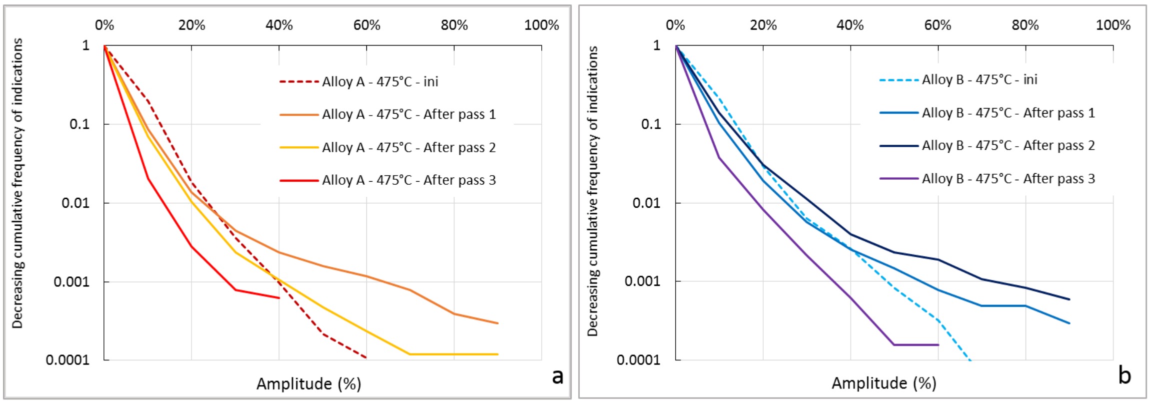

Figure 7. Quantitative treatment of HR-UT C-scans: decreasing cumulative frequency of indications for alloy A (a) and alloy B (b) deformed at 475°C. “Ini” refers to the initial level of indications – dotted lines.

Data can also be analyzed by choosing a given amplitude threshold and plotting the evolution of the frequency of indications above this threshold along the width of the specimen (moving average over a distance of 2.8 mm). Such type of results is given in Figure 9. Depending on the amplitude threshold pores of different sizes are taken into account. The beneficial effect of lowering the deformation temperature for alloy B on damage at the center is visible whatever the amplitude threshold chosen (see plot of Figure 8a). The curve corresponding to the sample deformed at 475°C from 50 to 33 mm thickness lies below the curve for 495°C and the same reduction, but above the curve representing initial quality (black dotted line in Figure 8).

When comparing alloy B to alloy A after the two first passes, a slight decrease in the frequency of indications is observed for alloy A in comparison with alloy B at the specimen center when the amplitude threshold is set to 10%. However no significant effect is seen at the edge whatever the deformation temperature (see Figure 9a). When the threshold is increased to 40% in order to consider only the large voids, the difference between the two alloys become more visible at the edge with a maximum frequency for alloy B nearly doubled in comparison with alloy A when deformation occurs at 495°C (see Figure 9b). However the initial quality of the samples were not perfectly identical, with alloy B having a slightly higher level of indications whatever the amplitude considered.

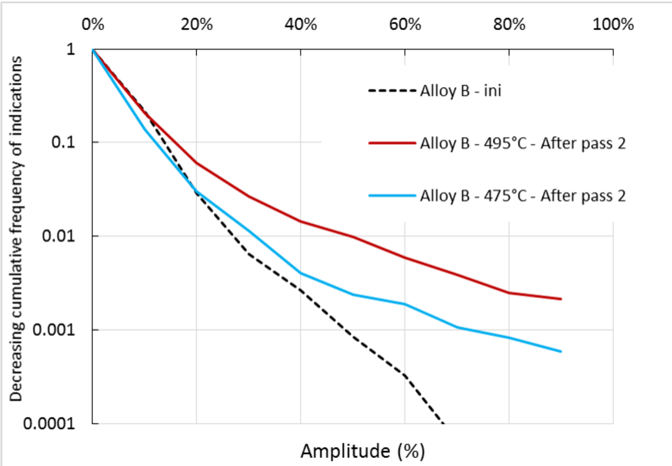

Figure 8. Effect of deformation temperature for alloy B: frequency of indications at the center of the specimen for the different amplitude thresholds

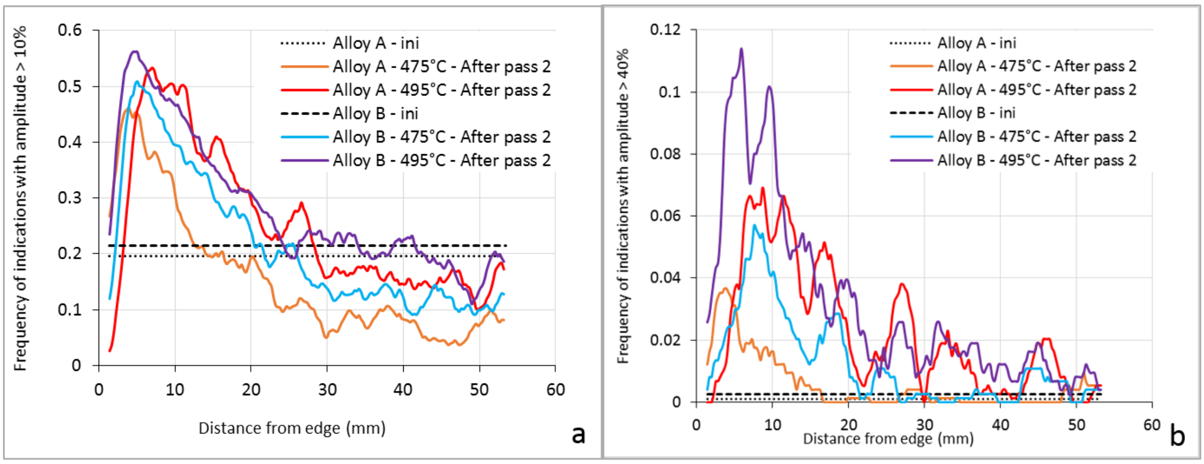

Figure 9. Comparison alloy A vs. alloy B in terms of profile along the specimen width: a) Indications above 10% amplitude b) Indications above 40% amplitude.

DISCUSSION AND CONCLUSIONS

In the present work, the well-known STT test has been applied on AlCuLi alloys of the 2050 family. In comparison with previously generated data on 7xxx alloys, 2050-type alloys display a higher maximum ductility and their ductility loss occurs at a higher temperature. Data for 7075 alloy are available in (Duly, 1998) where a sharp drop is visible at 450°C whatever the strain rate tested. The STT test is well discriminating, thanks to a good reproducibility, but the imposed deformation remains far below what is experienced in hot rolling. The Plane Strain Compression test (with low a/h) shows the important attribute of being able to increase the porosity level by deformation as can be experienced during hot rolling. This can best be evidenced by using HR-UT which allows mapping the distribution of voids contained in a large volume. The evolution of damage is dependent on the stress state, i.e. more depressive towards the edges, and temperature, i.e. less damage at lower temperature in the investigated range. This last point is in agreement with the observations of Harnish et al. who performed hot uniaxial compression tests over a wide range of temperatures and strain rates on 7000 alloys (Harnish, 2005). The onset of localized damage at the grain boundaries was detected at a temperature of 455°C by post-mortem SEM observations. During compression at 500°C, of these 7000 alloy samples, multiple voids even coalesced to give rise to an elongated crack. Inter-granular sliding is known to appear above a strain rate-dependent critical temperature when the grain boundaries fail at a low stress compared to the grain interior flow stress (Sainfort, 1975). This phenomenon makes plastic deformation easier but adversely leads to fracture along the grain boundaries, mostly at interfaces between inter-granular precipitates and the matrix.

Figure 10 compares the results obtained with the STT test with those obtained with the PSC test at high h/a ratio. Both tests give a similar trend on the detrimental effect of increasing the temperature on the damage evolution, for both alloys. Alloy A appears however less sensitive to the deformation temperature. Without affecting the ductility very much at 475°C, vanadium addition increases the porosity level after deformation (note that the initial porosity is marginally different in the initial state). Shi and Chen (2014, 2016) studied the effect of vanadium and zirconium additions in 7150 on hot deformation behavior. Their tests conditions are somewhat different from the present: axial compression is used, at lower temperatures (300–450°C) and the focus is on smaller strain rates. They showed that vanadium is essentially in solid solution up to 500 ppm. It increases the resistance to recovery and promotes damage formation at grain boundaries (Shi, 2014). The interpretation from the authors is that by limiting recovery, vanadium effectively enhances the stresses on grain boundaries, dynamic recrystallization not being able to compensate for this effect. The creation of damage is associated with a zone of high dissipation in the processing maps, developed to identify the optimum hot working conditions. Processing maps combine the calculated efficiency of power dissipation with a flow instability criterion. Li et al. have evidenced two instability domains in these maps at high strain rates for an Al-3.5%Cu-1.5%Li-0.1%Sc-0.12%Zr alloy: the first one between 380 and 420°C for a strain rate in the range 0.1–10 s^{-1}, the second one at 460–500°C with a strain rate of 0.3–10 s^{-1} (Li, 2014).

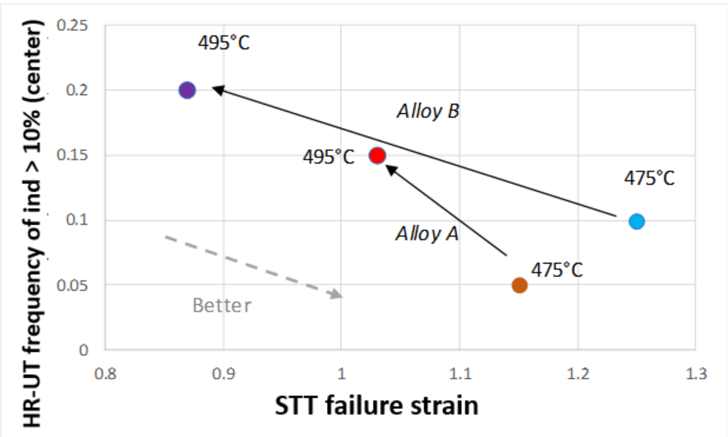

Figure 10. Synthesis of STT and PSC results for both alloys A and B tested at 475 and 495°C.

The novelty of the present study is the link between deformation conditions close to those experienced during industrial hot-rolling of thick plates and damage development quantification. This has been made possible thanks to the combination of an appropriate PSC experiment with low a/h ratios and high-resolution ultrasonic scans of the deformed regions. In order to go further in terms of damage quantification, the correlation between HR-UT amplitude and pore size should be established. X-ray tomography can be a useful tool to achieve this goal. In addition to size, initial pore morphology and its orientation during the course of deformation may influence both HR-UT signal and the closure efficiency.

REFERENCES

Chéhab, B., Bréchet, Y., Glez, J.-C., Jacques, P., Mithieux, J.-D., Véron, M., & Pardoen, T. (2006). Characterization of the high temperature tearing resistance using the essential work of fracture - Application to dual phase ferritic stainless steels. *Scripta Materialia*, *55*(11), 999-1002.

Duly, D., Lenard, J., & Schey, J. (1998). Applicability of indentation tests to assess ductility in the hot-rolling of aluminium alloys. *Journal of Materails Processing Technology, 75*(1), 143-151.

Ehrström, J.-C. (1989). *Alliages Al-Fe-X élaborés par métallurgie des poudres: microstructure, comportement et endommagement.* PhD, Ecole des Mines de Paris.

Harnish, S., Padilla, H., Gore, B., Dantzig, J., Beaudoin, A., Robertson, I., & Weiland, H. (2005). High temperature mechanical behavior and hot-rolling of AA705X. *Metallurgical and Materials Transactions*, 357-369.

Lequeu, P., Smith, K., & Daniélou, A. (2010). Aluminium-copper-lithium alloy 2050 developed for medium to thick plate. *Journal of Materials Engineering and Performance, 19*(6), 841-847.

Li, B., Pan, Q., & Yin, Z. (2014). Characterization of hot deformation behavior of as-homogenized Al-Cu-Li-Sc-Zr alloy using processing maps. *Materials Science and Engineering A*, 199-206.

Ratchev, P., Verlinden, B., P., V. H., & P., D. S. (1997). Hot ductility of an Al-4wt.%Mg-0.5wt.%Cu alloy. *Materials Science and Engineering*, 189-196.

Saby, M., Bouchard, P.-O., & Bernacki, M. (2014). Void closure criteria for hot metal forming: A review. *Journal of Manufacturing Processes, 19*, 239-250.

Sainfort, G. (1975). Comportement à chaud des métaux et alliages. *Mise en forme des Métaux et Alliages* (pp. 87-98). Villards-sur-Ollon, Suisse: CNRS.

Schey, J., & Woodall, S. (1979). Development of new workability test techniques. *Journal of Mechanical Working Technology, 2*(4), 367-384.

Shi, C. (2014). *Effects of Zr and V on microstructure and hot deformation behavior of 7150 alloys.* PhD University of Quebec.

Shi, C., & Chen, X.-G. (2014). Effect of vanadium on hot deformation and microstructural evolution of 7150 aluminum alloy. *Materials Science and Engineering*, 91-102.

Shi, C., & Chen, X.-G. (2016). Evolution of activation energies for hot deformation of 7150 aluminum alloys with various Zr and V additions. *Materials Science and Engineering*, 197-209.

Thomson, P., & Burman, N. (1980). Edge cracking in hot-rolled Al-Mg alloys. *Materials Science and Engineering, 45*(1), 95-107.

Timothy, S., Yiu, H., Fine, J., & Ricks, R. (1991). Simulation of single pass of hot rolling deformation of aluminium alloy by plane strain compression. *Materials Science and Technology, 7*, 255-261.